JOURNAL OF MATERIALS SCIENCE 6 (1971) 1367-1378

Clustering and Solute-Vacancy Binding Energies in Al-4.4% Zn Alloy with 0.01% Ternary Additions

K. S. RAMAN, E. S. D. DAS, K. I. VASU
Materials Research Group, Department of Metallurgy, Indian Institute of Science, Bangalore-12, India

Isochronal and isothermal ageing experiments have been carried out to determine the influence of 0.01 at. % addition of a second solute on the clustering rate in the quenched Al-4.4 a/o Zn alloy. The influence of quenching and ageing temperatures has been interpreted to obtain the apparent vacancy formation and vacancy migration energies in the various ternary alloys. Using a vacancy-aided clustering model the following values of binding free energy have been evaluated: Ce – 0.18; Dy – 0.24; Fe – 0.18; Li – 0.25; Mn – 0.27; Nb – 0.18; Pt – 0.23; Sb – 0.21; Si – 0.30; Y – 0.25; and Yb – 0.23 (± 0.02 eV). These binding energy values refer to that between a solute atom and a single vacancy. The values of vacancy migration energy (*c.* 0.4 eV) and the experimental activation energy for solute diffusion (*c.* 1.1 eV) are unaffected by the presence of the ternary atoms in the Al-Zn alloy.

1. Introduction

The presence of trace elements or impurities plays a very important rôle in the decomposition of quenched, supersaturated solid solutions. The presence of impurities also produces a significant and measurable influence on the rate of resistivity change during ageing; this has been advantageously used for computing the solute-vacancy binding energies in alloys. Although this is an indirect method, it has been shown to yield reliable values of binding energy that are of particular interest in the interpretation of the ageing kinetics and solute diffusion in quenched alloys. The solute-vacancy binding energies have been determined for a number of solutes in different solvent matrices. The trace elements have a strong influence on the ageing characteristics of binary alloys. They may: (i) modify the interfacial energy between a precipitate particle and the matrix; (ii) change the free energy relationships in an alloy system so that precipitation of a different phase is favoured; (iii) segregate to grain boundaries and inhibit discontinuous precipitation; (iv) increase solute supersaturation at the ageing temperature; (v) stabilise vacancy clusters and inhibit the formation of denuded zones in the vicinity of grain boundaries, with a consequent improvement in stress-corrosion resistance; and (vi) promote uniform fine precipitation.

The vacancy-binding free energies (subsequently termed vacancy binding energies) for a number of solutes have been determined by measuring the slowing down effect in the ageing rate in Al-Cu, Al-Zn and Al-Mg alloys. The present investigation deals with the rôle of trace elements on the clustering characteristics of an Al-4.4% Zn (all compositions in the text and tables are given in at. % only), and to evaluate the solute-vacancy binding energies. For this purpose the following experimental conditions were studied:

(*a*) isochronal ageing behaviour of quenched alloys;

(*b*) dependency of quenched-in-resistivity on quenching temperature;

(*c*) influence of quenching and ageing temperatures on the isothermal ageing characteristics.

2. General Approach

The clustering process was followed by measuring the changes in electrical resistivity during ageing. The quenched-in-resistivity ($\Delta\rho_q$), time-to-peak (t_m) and the initial ageing rate (dR/dt) were the parameters used to derive the kinetics of clustering.

The total vacancy concentration (atom fraction) C_v^b, in the Al-Zn alloy can be expressed as [1]:

$$C_v^b = A(1 - 12C_{Zn} + 12C_{Zn}.\exp(E_B^{v-Zn}/kT_q) \exp(-E_f/kT_q) \quad (1)$$

$$C_v^b = A_o^b \exp(-E_f^b/kT_q) \quad (2)$$

where E_B^{v-Zn} is the v – Zn binding energy, T_q the quenching temperature, E_f the vacancy formation energy in aluminium, E_f^b the apparent vacancy formation energy in the alloy and A_o^b a constant containing an entropy term. The derivation of the above equation assumes the presence of only isolated mono-vacancies, solute atoms and solute-vacancy pairs, so that vacancy clustering, solute clustering and higher order solute-vacancy clustering are neglected. Also, the entropy term is assumed the same for free and associated sites.

If zinc atoms do not interact with atoms of a third element, then Lomer's [1] equation for the equilibrium vacancy concentration in the ternary alloy, C_v^t, can be written as:

$$C_v^t = A(1 - 12C_{Zn} + 12C_{Zn}\exp(E_B^{v-Zn}/kT_q) - 12C_i + 12C_i\exp(E_B^{v-i}/kT_q)) \times (\exp(-E_f/kT_q)) \quad (3)$$

$$C_v^t = A_o^t \exp(-E_f^t/kT_q) \quad (4)$$

where, C_i is the atom fraction of the ternary solute and E_f^t is the apparent vacancy formation energy in the ternary alloy. If the times to reach the peak in resistivity or the initial rate of ageing in the binary and the ternary alloys are considered, the ratio of C_v^t to C_v^b can be used to compute E_B^{v-i}, the vacancy-trace element binding energy.

From equations (1) to (4):

$$\text{Ageing Ratio} = \frac{C_v^t}{C_v^b} = \frac{A_o^t \exp(-E_f^t/kT_q)}{A_o^b \exp(-E_f^b/kT_q)} = \frac{(\text{time-to-peak})_{\text{binary}}}{(\text{time-to-peak})_{\text{ternary}}} = \frac{(\text{Initial ageing rate})_{\text{ternary}}}{(\text{Initial ageing rate})_{\text{binary}}}$$

$$= \frac{(1 - 12C_{Zn} + 12C_{Zn}\exp(E_B^{v-Zn}/kT_a) - 12C_i + 12C_i\exp(E_B^{v-i}/kT_a))}{(1 - 12C_{Zn} + 12C_{Zn}\exp(E_B^{v-Zn}/kT_a))} \quad (5)$$

This relation, evaluated at the ageing temperature T_a, helps to determine the vacancy-solute atom binding energy, by measuring the relative retardation brought about by the ternary atom. In deriving the above equation, it has been assumed that the fraction of vacancies in sites associated with binary as well as ternary solute atoms increases as the temperature falls from T_q to T_a. If E_B^{v-Zn} and E_B^{v-i} are not very small, the redistribution will occur very quickly, practically immediately after quenching [2-4].

An "effective binding energy" [2], between zinc atoms and vacancies in the concentrated Al-Zn alloy can be evaluated and used for computing the binding energy between the trace element and vacancies.

3. Experimental

Alloys were made using super-purity aluminium (99.997+) and high purity zinc (99.99+). Other alloy additions were made using metals of 99.9% or better purity. Alloy preparation procedure, their thermal and mechanical treatments and the specimen design employed have been discussed elsewhere [5, 6]. Ternary alloy additions were so calculated as to result in a 0.01% addition in the Al-4.4% Zn alloy. Table I gives the composition of the alloys used in this investigation.

TABLE I Alloy compositions used in the present investigation

Alloying element	Wt equivalent of 0.01 at. %	wt % Zinc* in the alloy
—	—	10.03
Cerium	0.045	10.10
Dysprosium	0.053	10.00
Iron	0.053	10.00
Lithium	0.0023	10.00
Manganese	0.0091	9.99
Niobium	0.03	10.01
Platinum	0.060	10.00
Antimony	0.040	10.00
Silicon	0.018	10.00
Yttrium	0.030	9.98
Ytterbium	0.056	9.99

*only in this table are wt % values given.

Specimens in the form of helical coils were first stabilised, then solutionised for 1 h at the desired quenching temperature, quenched into stirred ice/water bath at 0°C and immediately transferred into the liquid air bath. After measuring the resistivity at this temperature (to obtain $\Delta\rho_q$), the specimen was transferred to the ageing bath, and the resistivity changes were recorded directly at the ageing temperature.

4. Results and Analysis

Results are presented here in terms of resistivity increments in n Ω cm units (= 10^{-9} ohm/cm),

over a pre-selected reference state. For obtaining the reference resistivity the samples were homogenised at a temperature of 200°C (just above the solvus temperature for the alloys) and quenched, and the resistivity measurements were made at respective ageing temperatures to obtain the appropriate value of the reference resistivity. This treatment is expected to produce a condition of random distribution of solute atoms, and no appreciable cluster formation due to the very low concentration of vacancies quenched-in from this temperature. It was also found that the reference resistivities measured by this method were very nearly the same as the ones obtained from the aged and fully reverted specimens. The resistivity change $\Delta\rho$ was obtained from the relation:

$$\Delta\rho = \rho_0(R_t - R_0)/R_0 \qquad (6)$$

where ρ_0 and R_0 are the resistivity and the resistance of the sample respectively, in the reference state.

Fig. 1 shows the resistivity changes during isochronal annealing of the alloys after quench from a temperature of 380°C. Isochronal ageing was carried out for 2 min. intervals at each temperature, in steps of 20°C in the range − 80 to 200°C. Resistivity measurements were made at liquid air temperature. This set of experiments was carried out to gain a qualitative understanding of the nature of alloy decomposition. The general pattern of the isochronal curves for the ternary alloys is similar to that for the base binary alloy. It is found that in the range − 80 to 20°C, the resistivity increases to a peak followed by a continuous decrease to a plateau; in certain cases, a second decrease is observed at higher temperatures.

Figs. 2a-k show the resistivity changes during isothermal ageing at 0°C after quench from different indicated temperatures. These results are typical of measurements at different ageing temperatures, which are not included here. From the shapes of the isothermal curves it can be observed that the zone forming process takes place by the same mechanism in all the alloys, and there appears to be no nucleation barrier for this process. The presence of 0.01% of the ternary addition does not influence the scale of zone formation, as can be seen from the nearly equal peak-heights in resistivity, which is independent of the quenching temperature, in all the alloys.

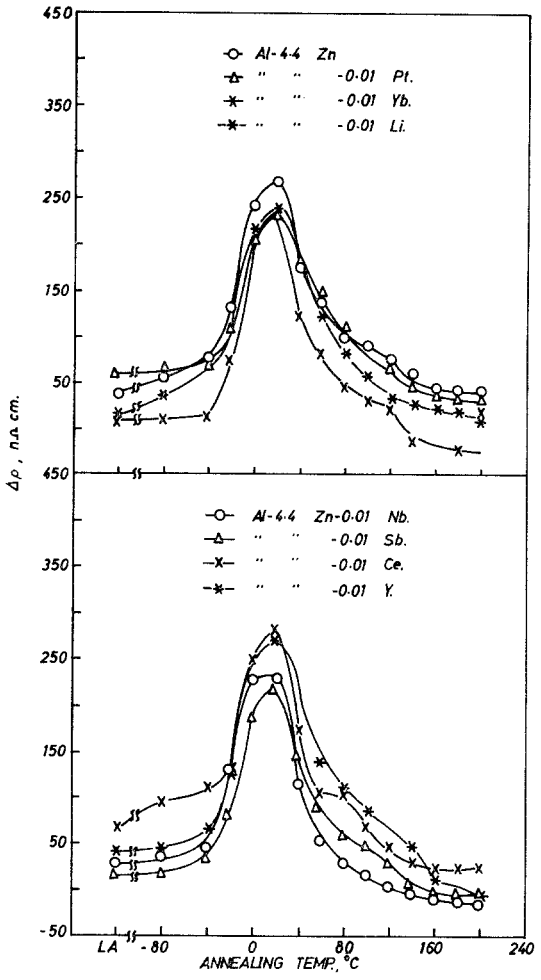

Figure 1 Resistivity changes during isochronal annealing of some of the alloys studied after quench from 380°C. (2 min. anneals taken at 20°C intervals).

4.1. Time-to-peak in Resistivity

Using the peak in resistivity to represent an identical state of zone distribution in the alloy for different quenching temperatures, t_m can be related to the associated activation energy through the equation:

$$t_m = t_0.\exp(E_f/kT_q) \qquad (7)$$

The Arrhenius plots relating $\log(t_m)$ and $1/T_q$ are drawn in fig. 3 and the values of the apparent activation energy for formation of vacancies derived therefrom, for the different alloys have been tabulated in table II.

Before the above values of the vacancy formation energy can be used in quantitative calculations, they need be corrected for two

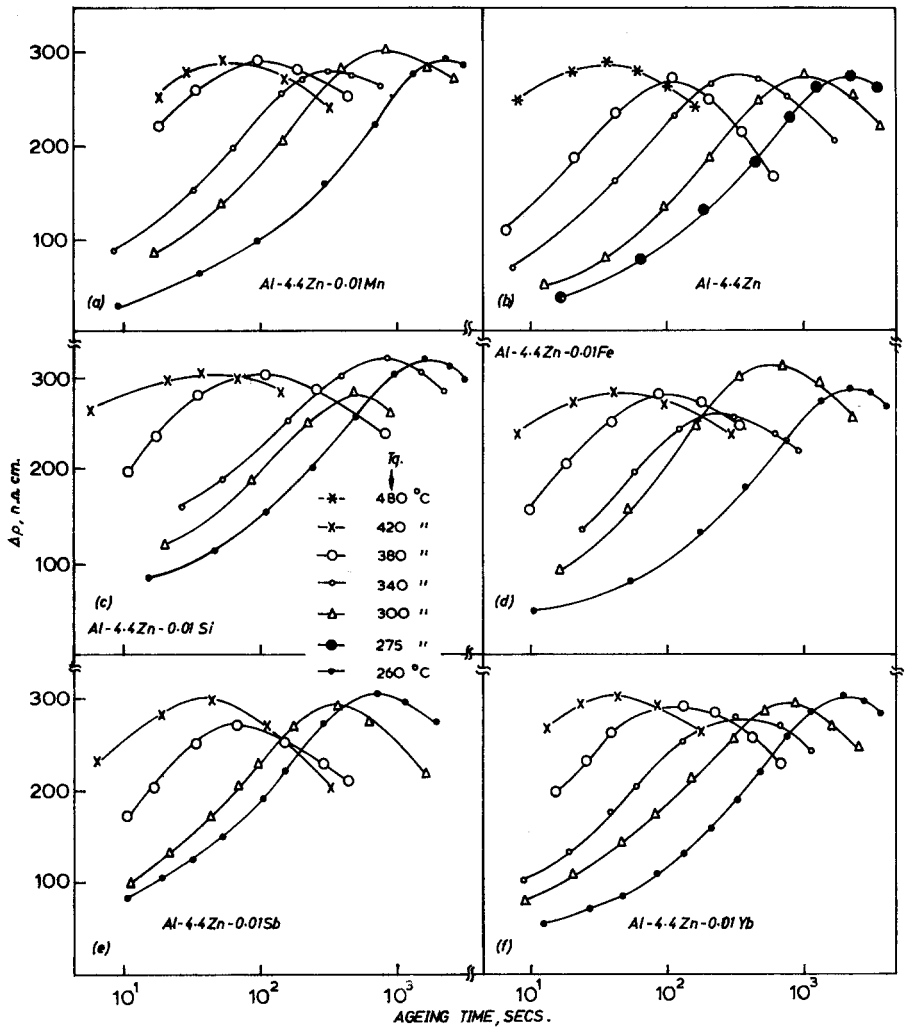

Figure 2 Isothermal resistivity changes at 0° C in the alloys studied after quench from different temperatures.

significant effects, viz., (i) effect of solute depletion due to zone formation, on the vacancy environment in the matrix during the time interval elapsed between quenching and the appearance of the peak in resistivity, and (ii) the influence of the ternary element on the vacancy life time in the alloy matrix. Both these corrections have been applied based on the method suggested by Perry [2] and the corrected values of vacancy formation energy so obtained are also included in table II.

4.2. Initial Ageing Rate

In order to evaluate the initial ageing rate, many methods have been used [2, 7]. In the present case, the experimental data were programmed on an IBM 7044 computer to determine the best fitting polynomial. The values of the initial ageing rate were then obtained by putting zero time in the rate equation. Without exception, the results of curve fitting were 3rd degree polynomials, yielding a quadratic rate equation of the type:

$$dR/dt = a + bt + ct^2 \qquad (8)$$

This agrees well with a similar equation used by Perry [2] for the ageing data on Al-Zn and Al-Zn-Mg alloys. Using the values of dR/dt at $t = 0$, as a function of T_q, the values of the apparent vacancy formation energy were calculated in a way similar to that used with the time-to-peak data, and are given in table II. It may be

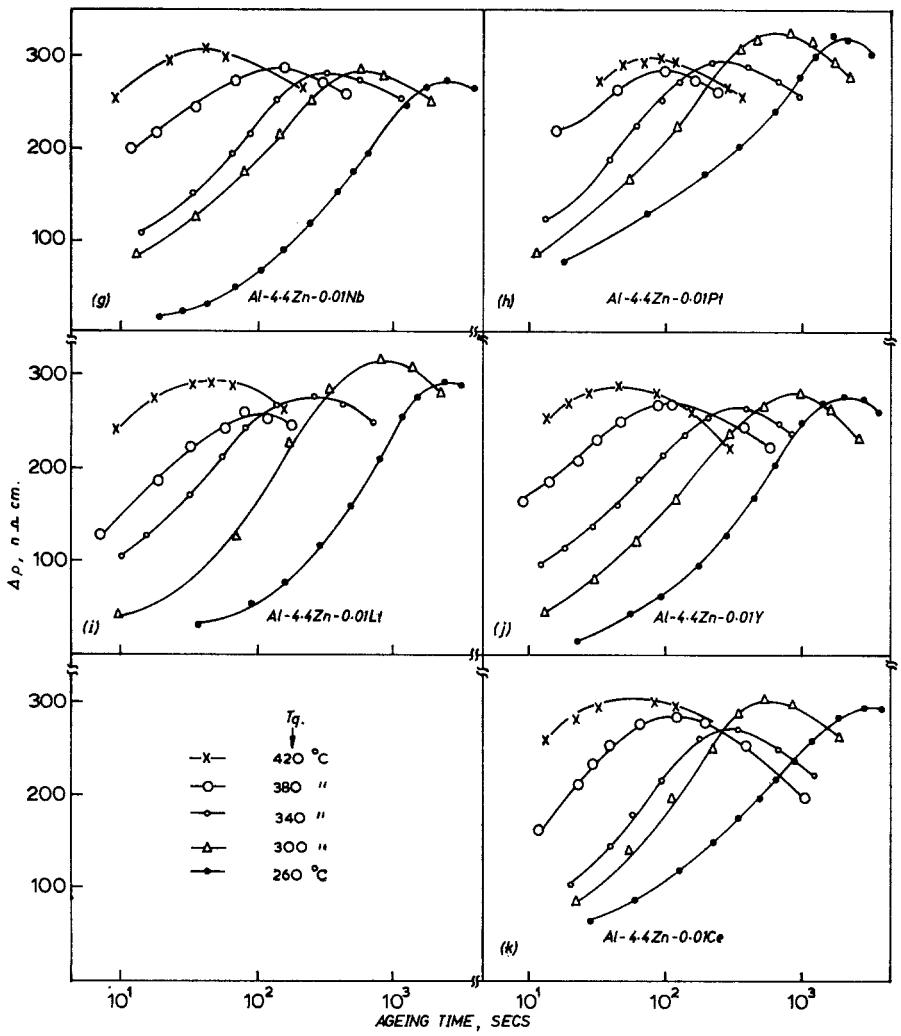

Figure 2 (continued).

observed that the values obtained by the two methods are close to each other.

A similar evaluation made by considering the dependency on T_a, of either t_m or dR/dt would yield the apparent activation energy for migration of vacancies. These values have been calculated and included in table III, and the related activation plots are shown in fig. 4. It may be observed that these plots are not strictly linear in the entire range of temperatures studied, but are made up of two linear portions, one for T_a below 20°C, and the other for temperatures above 20°C. The high temperature portion has more or less the same slope for all the alloys, corresponding to an activation energy of about 0.2 eV. A similar variation had been observed in the Al-Zn alloys [8].

The values of E_f^t evaluated above may be substituted in equation 5 to obtain the values of E_B^{v-i} (table II). For this purpose a value of 0.06 eV [8] has been used for the vacancy-zinc binding energy.

4.3 Ageing Ratio

The values of binding energy may be computed by using the experimental ageing ratios also; ageing ratio can be calculated from time-to-peak as well as initial ageing rate data. For this purpose only results obtained for ageing at 0°C have been used to demonstrate the applicability of the ageing ratio method. The ageing ratios were computed (*a*) directly from the time-to-peak

TABLE II Values of apparent vacancy formation energy in the various alloys studied, and the solute-vacancy binding energies

Alloy	Vacancy Formation Energy, eV			E_B^{v-i}* (± 0.02 eV)
	from time-to-peak		from initial ageing rates	
	Uncorrected	corrected		
Al-4.4 Zn	0.81	0.70	0.66	
Al-4.4 Zn-0.01 Ce	0.80	0.69	0.69	0.18
Al-4.4 Zn-0.01 Dy	0.77	0.66	0.66	0.24
Al-4.4 Zn-0.01 Fe	0.75	0.69	0.69	0.18
Al-4.4 Zn-0.01 Li	0.76	0.64	0.63	0.26
Al-4.4 Zn-0.01 Mn	0.69	0.62	0.63	0.27
Al-4.4 Zn-0.01 Nb	0.82	0.69	0.70	0.18
Al-4.4 Zn-0.01 Pt	0.78	0.67	0.67	0.23
Al-4.4 Zn-0.01 Sb	0.80	0.68	0.68	0.21
Al-4.4 Zn-0.01 Si	0.77	0.60	0.60	0.30
Al-4.4 Zn-0.01 Y	0.76	0.65	0.64	0.25
Al-4.4 Zn-0.01 Yb	0.78	0.67	0.67	0.23

*Values calculated using equation (5), with a value of 0.06 eV for E_B^{v-Zn}.

TABLE III Values of apparent vacancy migration energies in the various alloys investigated

	Vacancy Migration Energy, eV for ageing below 20° C						Vacancy migration energy for ageing above 20° C
	T_q = 260° C			T_q = 300° C			
	(1)	(2)	(3)	(1)	(2)	(3)	eV
Al-Zn	0.42	0.42	0.43	0.40	0.40	0.40	0.23
Al-Zn-Ce	0.47	0.46	0.42	0.45	0.44	0.44	0.20
Al-Zn-Dy	0.41	0.41	0.42	0.39	0.40	0.40	0.22
Al-Zn-Fe	0.44	0.42	0.43	0.39	0.39	0.40	0.25
Al-Zn-Li	0.40	0.40	0.40	0.37	0.37	0.37	0.22
Al-Zn-Mn	0.44	0.44	0.43	0.40	0.38	0.39	—
Al-Zn-Nb	0.47	0.45	0.45	0.41	0.40	0.40	0.20
Al-Zn-Pt	0.46	0.44	0.44	0.44	0.43	0.43	—
Al-Zn-Sb	0.45	0.42	0.42	0.42	0.40	0.40	0.20
Al-Zn-Si	0.39	0.37	0.39	0.35	0.35	0.37	0.24
Al-Zn-Y	0.44	0.41	0.40	0.39	0.38	0.37	0.22
Al-Zn-Yb	0.41	0.40	0.42	0.38	0.38	0.39	0.17

(1) Values from time-to-peak, uncorrected; (2) Values from time-to-peak, corrected; (3) Values from initial ageing rate data.

TABLE IV Experimental ageing ratios obtained from time-to-peak data in the alloys studied and the corresponding vacancy-solute binding energies

Alloy used	Ageing ratios at 0°C after quench from 300°C		340°C		380°C		Average AR_0	E_B^{v-i} (± 0.02 eV)
	AR	AR_0	AR	AR_0	AR	AR_0		
Al-Zn-Ce	1.08	1.12	1.10	1.14	1.12	1.14	1.13	0.18
Al-Zn-Fe	1.00	1.13	1.00	1.13	1.12	1.12	1.13	0.18
Al-Zn-Li	1.71	1.98	1.80	2.01	1.83	2.04	2.01	0.26
Al-Zn-Mn	1.25	1.86	1.25	1.88	1.26	1.84	1.86	0.25
Al-Zn-Nb	1.05	1.13	1.10	1.13	1.12	1.13	1.13	0.18
Al-Zn-Pt	1.41	1.60	1.53	1.63	1.60	1.60	1.61	0.23
Al-Zn-Sb	1.20	1.38	—	—	1.26	1.38	1.38	0.21
Al-Zn-Si	1.35	2.30	1.33	2.32	1.42	2.30	2.31	0.28
Al-Zn-Y	—	—	1.66	1.88	1.70	1.86	1.87	0.25
Al-Zn-Yb	1.42	1.62	1.44	1.62	1.50	1.60	1.61	0.23

Note: 1. AR : Ageing ratio obtained from time-to-peak data
2. AR_0: Ageing ratio obtained by extrapolation to zero ageing time [2]
3. E_B^{v-i} obtained by using equation (5).

data, which were corrected to obtain the extrapolated [2] value at zero ageing time; or (*b*) from the initial ageing rate data. As can be seen from table IV these values agree well with each other. By using equation 5 the values of E_B^{v-i} have been evaluated in the various alloys (except the Al-Zn-Dy alloy) using the corresponding values of the ageing ratios (table IV).

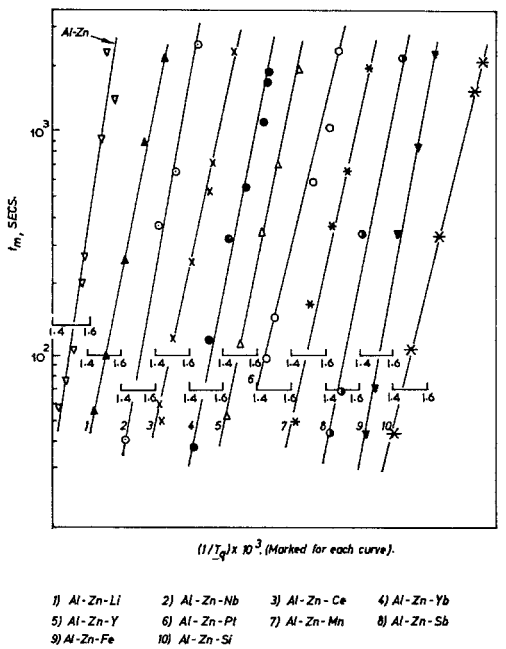

Figure 3 Activation plots relating $\log(t_m)$ with reciprocal quenching temperatures for the various alloys studied.

5. Discussion of Results

Reference to fig. 1 indicates that for identical conditions of ageing, the time-to-peak is larger in all the ternary alloys than in the binary Al-4.4 Zn alloy. This is a definite indication of the interaction between the ternary solute and the quenched-in vacancies. This inference is based on a vacancy-aided mechanism for the growth of clusters, and the temporary loss of vacancies by the formation of ternary atom-vacancy couples, which are considered to be less mobile. If the ternary solute strongly interacts with vacancies, but does not migrate to zones, then the lattice vacancies are trapped and there occurs a decrease in the zinc clustering rate. However, if the solute is a zone-forming constituent and acquires an associated vacancy, its migration rate will be high. Both the solutes will then be transported simultaneously through the

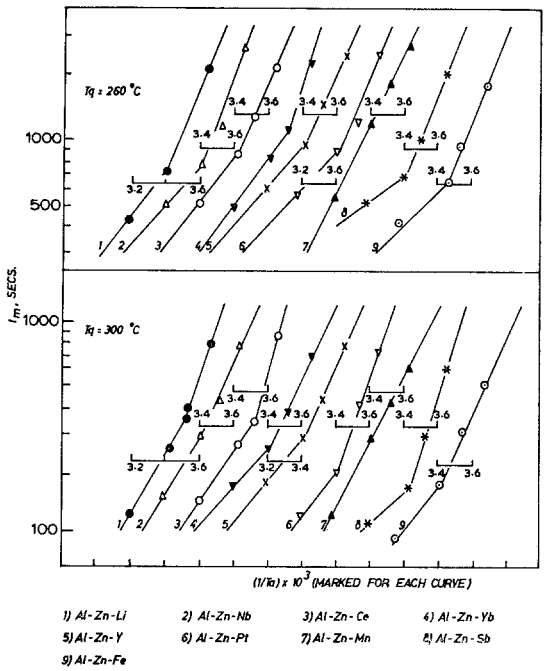

Figure 4 Arrhenius plots of $\log(t_m)$ versus reciprocal ageing temperature for the various alloys studied.

formation of clusters comprising atoms of zinc and the second solute, and an associated vacancy, which migrate to zones by continual interchange of the vacancy between the cluster constituents and the surrounding solute atoms. In this case there is observed an acceleration in the clustering rate. Such a case has been experimentally realised in Al-Zn-Ag alloys quenched from lower temperatures [6]. In the present series of alloys, therefore, a reasonable assumption can be made that the ternary elemental additions are not zone-forming constituents, but they only trap vacancies giving rise to the observed retardation in the zinc clustering rate. The magnitude of the interaction energy for the formation of the solute-vacancy pair can therefore be evaluated by measuring the relative ageing rates in the binary and ternary alloys under identical conditions of quenching and ageing.

It has been shown that in the Al-4.4 Zn alloy, zinc atoms exhibit an effective binding energy of 0.06 eV [2, 8]. In order to arrive at a simple picture of the relative vacancy concentration, it may be assumed as a first approximation, that the value of 0.06 eV is small enough to be neglected. The vacancy concentration in the binary alloy will then be simply equal to that in

pure aluminium quenched from the same temperature. For quenching temperatures employed here, viz., 250 to 450°C, this value is in the range 5×10^{-7} to 3×10^{-5}. Thus the vacancy concentration is 1 to 3 orders of magnitude lower than the ternary solute concentration of 10^{-4} in the ternary alloys. This would mean that the existence of complexes with more than one vacancy can be ignored.

Again, if the field of solute-vacancy interaction does not extend beyond nearest neighbour sites, and the vibrational entropy is unchanged near a solute atom, then the fraction C_p, of associated vacancies will be:

$$C_p = \frac{12C_i\, C_v \exp(E_B^{v-i}/kT)}{1 + C_v \exp(E_B^{v-i}/kT)} \qquad (9)$$

Allowing a maximum of one vacancy per solute, all the solute atoms will be associated if,

$$12C_i\, C_v \exp(E_B^{v-i}/kT = 1 + C_v \exp(E_B^{v-i}/kT) \quad \ldots\ldots (10)$$

At a temperature of 450°C, E_B^{v-i} has to be *c.* 0.5 eV for all the solute atoms to be associated. Available estimates of binding energy are well below 0.5 eV and hence in all the ternary alloys studied, there will be a good proportion of solute atoms without an associated vacancy. If allowance is now made for the positive binding between zinc atoms and vacancies, it will simply result in a redistributuion of vacancies between zinc and the ternary solute atoms. In all the ternary alloys, therefore, the existence of simple solute-vacancy pairs is justified, and the evaluated solute-vacancy binding energies are reliable estimates for binding between a single solute atom and a single vacancy.

5.1. Magnitude of Solute-Vacancy Binding Energy

In the foregoing sections an attempt has been made to interpret the observed resistivity changes in terms of preferential vacancy-binding by ternary solutes, within the limitations associated with the use of the modified Lomer's equations. These estimates have been compared with other experimental values available in literature in table V.

The various ternary additions, whose influence has been reported herein, were selected on the basis of the following reasons:
(*a*) those for which reliable binding energy data were not available;
(*b*) those for which good estimates were available, e.g. Si; to serve as a check for the method of evaluation used here.

Values of binding energy used in table V for comparison include:
(i) equilibrium measurements made at high temperatures;
(ii) measurements on quenched metastable alloys;
(iii) theoretical estimates.

Since theories are not yet developed to a stage when they can fully explain the significance of the Binding Energy, a comparison with these estimated values is not fully justified. In making comparisons between values from (i) and (ii) above, the greatest difference due to the temperature effect is approximately 0.02 eV, which is of the same order of magnitude as the error in the experimental estimation here.

5.1.1. Iron

The value of 0.18 eV derived here agrees well with that measured by Perry and Entwistle [9] by investigating into the slowing down effect of iron addition in an Al-Cu alloy. The good agreement is perhaps due to the fact that both the estimates have been made by identical methods.

5.1.2. Manganese

The present value of 0.27 eV for the vacancy-manganese binding energy is slightly higher than those reported in literature [9-12].

5.1.3. Silicon

This element has been very widely studied perhaps because of its commercial importance. King and Burke [17] reported a value of 0.2 eV for the v-Si binding energy from their high temperature, equilibrium measurements. Normally, as reported by Beaman *et al* for the v-Ag binding energy of 0.08 eV [21], and for v-Mg binding energy of *c* 0.01 eV [22], the solute-vacancy binding energies estimated by high temperature equilibrium measurements are of the order of 0.01 to 0.08 eV. The quenching experiments as well as the high temperature equilibrium measurements yield a higher value for the binding energy between silicon atoms and vacancies. This confirms that silicon atoms exhibit high binding energy to vacancies. This also affords an example wherein the high temperature equilibrium value is reasonably close to the values based on other methods of evaluation (table V). This agreement is taken to

TABLE V Comparison of solute-vacancy binding energies in aluminium matrix obtained by different methods

Element and alloy used	Method of evaluation	E_B^{v-i}, eV	Reference
Iron			
Al-4 Cu-0.01 Fe	Ageing Ratio	0.18	[9]
Al-4.4 Zn-0.01 Fe	Clustering	0.18	This work
Manganese			
Al-Zn-Mn	Ageing Ratio	0.23	[10, 11]
Al-4 Cu-0.01 Mn	Ageing Ratio	0.24	[9]
Al-Mn (dilute)	Quenched-in-resistivity	0.16	[12]
Al-4.4 Zn-0.01 Mn	Clustering	0.27	This work
Silicon			
Al-Si (002-0.15)	Specimen size effect	0.26	[13]
Al-4.4 Zn-0.1 Si	Clustering	0.15 to 0.27	[14]
Al-Zn-Si.	Ageing Ratio	0.28	[10]
Al-Si	Quenching	0.27	[15, 16]
Al-Cu-Si	Ageing Ratio	0.23	[9]
Al-Si	Lattice parameter	0.20	[17]
—	Theoretical	0.14, 0.25, 0.31	[18, 19, 20]
Al-4.4 Zn-0.01 Si	Clustering	0.30	This work
Cerium			
Al-4.4 Zn-0.01 Ce	Clustering	0.18	This work
Dysprosium			
Al-4.4 Zn-0.01 Dy	Clustering	0.24	This work
Lithium			
Al-4.4 Zn-0.01 Li	Clustering	0.26	This work
Niobium			
Al-4.4 Zn-0.01 Nb	Clustering	0.18	This work
Platinum			
Al-4.4 Zn-0.01 Pt	Clustering	0.23	This work
Antimony			
Al-4.4 Zn-0.01 Sb	Clustering	0.21	This work
Yttrium			
Al-4.4 Zn-0.01 Y	Clustering	0.25	This work
Ytterbium			
Al-4.4 Zn-0.01 Yb	Clustering	0.23	This work

be of significance as it supports the validity of the present mode of evaluation.

5.1.4. Dysprosium

The peak height for isothermal curves in the Al-Zn-Dy alloy increases with T_q (data presented and discussed elsewhere [23]) indicating a possible increase in the number of zones formed with T_q due to solute-solute type of interactions. The binding energy value given here for Dy is therefore subject to correction, and not reliable.

5.1.5. Other ternary solutes

For the other solutes, viz., Ce, Li, Nb, Pt, Sb, Y, and Yb, no other values of binding energy seem to be available for comparison with the present results. For reasons discussed earlier, values listed in table V are considered to be reliable estimates.

5.2. Elastic and Electronic Contributions to Vacancy-Solute Binding

The vacancy-solute interaction has been shown to arise out of two individual contributions: the electronic part [24] and the elastic part [25]. Though theoretical procedures are available to determine these contributions separately [24, 25], experimental methods for the same are lacking [10]. An attempt has been made here to determine the more predominant factor by listing the available estimates of binding energy in tables VI and VII for elements with similar valencies (considered to be zero for transitional elements) and similar sizes [26] respectively. Values obtained under nearly similar experimental conditions and methods of evaluation have been used in these tables.

5.2.1. Binding Energies of elements with similar valencies

Table VI shows that elements Fe, Mn, Dy, Ce, and Yb have atomic misfit parameters increasing from − 11.8 to + 35.3, but their respective binding energies do not show any regular variation. Similarly for the monovalent set of metals Cu, Au, Ag, and Li, the bivalent set Be, Zn, Cd, Mg, and Ca, and the tetravalent set Si, Ge, Ti, Zr, Sn, and Pb, all of which are arranged in the increasing order of atomic misfit with aluminium lattice, no regular variation in their

TABLE VI Comparison of vacancy-solute binding energy values for elements with similar valencies

Element	Valency	Misfit parameter $\frac{r_{Al} - r_i}{r_{Al}} \times 100$	E_B^{v-i} (eV)	Reference
Fe	0	− 11.8	0.18	This work
Mn	0	− 8.6	0.27	This work
Dy	0	+ 23.9	0.24	This work
Ce	0	+ 27.2	0.18	This work
Yb	0	+ 35.3	0.23	This work
Be	2	− 21.4	0.26	[27]
Zn	2	− 3.5	0.21	[9]
Cd	2	+ 7.8	0.32	[28]
Mg	2	+ 11.8	0.18	[2]
Ca	2	+ 38.5	0.27	[10]
Si	4	− 8.0	0.30	This work
Ge	4	− 4.4	0.33	[10]
Ti	4	+ 2.7	0.30	[10]
Zr	4	+ 11.8	0.33	[10]
Sn	4	+ 13.4	0.31	[29]
Pb	4	+ 22.2	0.38	[10]

binding energy values was observed. It can therefore be conceived that the elastic-interaction contribution to the solute-vacancy binding energy though present, might not play a major rôle.

5.2.2. Binding Energies of elements with similar sizes

For the elements Cu, Zn, Si, and Ge, which have similar sizes but different valencies, variation of binding energy with valency seems to be pronounced, particularly between Mn and Si, Zn and Ge, and Cu and Si. A similar observation may be made for the metals Mg and Zr, and Li and Cd. Again for Dy, Y, and Pb; Yb, Ce and Ca, and Fe and Be, a regular variation of binding energy with valency is observed. Thus the electronic contribution to the binding energy seems to be more pronounced than the elastic contribution, as was suggested by Shimizu and Takamura [30]. Any variation in the binding energy for elements belonging to the same group in the periodic table [10] may be due to the fact that these elements might exhibit a different effective valence in aluminium as distinct from

TABLE VII Comparison of vacancy-solute binding energy values for elements with similar sizes

Element	Valency	Misfit parameter $\frac{r_{Al} - r_i}{r_{Al}} \times 100$	E_B^{v-i} (eV)	Reference
Mn	0	− 8.6	0.27	This work
Cu	1	− 10.7	0.23	[10]
Zn	2	− 3.5	0.21	[9]
Si	4	− 8.0	0.30	This work
Ge	4	− 4.4	0.33	[10]
Pt	8	− 3.1	0.23	This work
Mg	2	+ 11.8	0.18	[2]
In	3	+ 16.2	0.39	[10]
Sn	4	+ 13.4	0.31	[29]
Zr	4	+ 11.8	0.33	[10]
Sb	5	+ 11.3	0.21	This work
Li	1	+ 8.4	0.26	This work
Cd	2	+ 7.8	0.32	[28]
Dy	0	+ 23.9	0.24	This work
Y	3	+ 25.8	0.25	This work
Pb	4	+ 22.2	0.38	[10]
Yb	0	+ 35.3	0.23	This work
Ce	0	+ 27.2	0.18	This work
Ca	2	+ 38.5	0.27	[10]

their group valency [31].

Therefore it can be summarised that the valency effect of vacancy-solute atom binding is very pronounced and the size effect, though observed in some cases, is smaller than the valence effect.

5.3. Experimental Activation Energy for Vacancy Migration and Solute Diffusion

The activation energy plots for vacancy migration show a break at 20°C for the binary alloy and the ternary additions (fig. 4) except Mn and Pt. The slope of the high temperature region corresponds to a vacancy migration energy of *c* 0.20 eV, and the low temperature portion of the activation plot yielded a vacancy migration energy of *c* 0.40 eV. This type of behaviour was also observed by Federighi [32] in pure aluminium. This can be associated with the growth process of zones. At lower temperatures (less than 20°C), zones can be considered to grow by the addition of single atoms [33]. At temperatures above 20°C, in addition to the movement of v-Zn pairs, the smaller zones might also migrate to the nearby growing larger zones [34]. Therefore it is necessary to use the migration energy computed from the low temperature portion of the activation plots (fig. 4) to calculate the activation energy for solute diffusion.

The values of migration energy for ternary alloys are nearly the same as for the binary alloy (*c* 0.4 eV), (table III). The apparent migration energy of zinc atoms is the effective migration energy of v-Zn pair, E_m, minus the v-Zn binding energy, E_B^{v-Zn} [35].

As the ternary additions are made in minute quantities and the cluster growth is mainly controlled by the movement of v-Zn pairs, the apparent migration energy is practically unaltered by ternary additions to the Al-4.4 Zn alloy. The values of vacancy migration energy measured therefore correspond to that of zinc atoms.

The experimental activation energy for zinc diffusion [32] in the different alloys can be calculated from the expression:

$$E_D = E_f + E_m + E_B^{v-Zn} \qquad (11)$$

This equation does not lead to a precise estimation of the experimental activation energy for zinc diffusion because the inter-relation between vacancy formation energies in the binary and the ternary alloys and v-Zn and v-i binding energies have not been taken into account. Further the data presented here are not adequate to make allowances for the temperature dependence of the impurity diffusion correlation factor. However, the values of activation energy for solute diffusion (*c* 1.10 eV) (table VIII) agree well with the value of Hilliard *et al* [36] and Beerwald [37], which is also around 1.1 eV. This confirms that the type of solute-vacancy complexes taking part in the solute diffusion is the same in all the alloys studied. In the initial stages of clustering of quenched alloys, solute diffusion is largely controlled by excess quenched-in vacancies via the formation of v-Zn complexes.

TABLE VIII Values of experimental activation energy for solute diffusion computed from the vacancy formation energy, vacancy migration energy and the vacancy-zinc binding energy

Alloy	VFE (± 0.01 eV)	VME (± 0.01 eV)	E_D (± 0.04 eV)
Al-Zn	0.70	0.45	1.21
Al-Zn-Ce	0.69	0.45	1.20
Al-Zn-Dy	0.66	0.41	1.13
Al-Zn-Fe	0.69	0.42	1.17
Al-Zn-Li	0.64	0.39	1.09
Al-Zn-Mn	0.62	0.37	1.05
Al-Zn-Nb	0.69	0.43	1.18
Al-Zn-Pt	0.67	0.44	1.17
Al-Zn-Sb	0.68	0.41	1.15
Al-Zn-Si	0.60	0.44	1.10
Al-Zn-Y	0.65	0.39	1.10
Al-Zn-Yb	0.67	0.40	1.13

E_D is computed from equation (11), for which a value of $E_B^{v-Zn} = 0.06$ eV has been used.

6. Conclusions

The foregoing discussions show that trace element additions exert a measurable influence on the kinetics of clustering in the Al-4.4% Zn alloy, although the general process of clustering remains unaltered. The following values of binding energy between a single vacancy and a solute atom, are obtained by interpretation of the results:

Ce – 0.18; Fe – 0.18; Li – 0.26; Mn – 0.27; Nb – 0.18; Pt – 0.23; Sb – 0.21; Si – 0.30; Y – 0.25; and Yb – 0.23 (± 0.02 eV).

The magnitudes of the binding energy evaluated seem to be more influenced by the valency difference than the difference in atomic sizes between the solute and aluminium atoms.

Acknowledgements

The authors are thankful to Dr S. Dhawan,

Director and Professor A. A. Krishnan for their interest in this work, and to other members of the Materials Research Group for their willing co-operation.

References

1. W. M. LOMER, in "Vacancies and other Point Defects in Metals and Alloys", (J. Inst. Met. Symp., London) (1958) 79.
2. A. J. PERRY, *Acta Metallurgica* **14** (1966) 1143.
3. M. OHTA and F. HASHIMOTO, *J. Phys. Soc. Japan* **19** (1964) 133.
4. A. J. PERRY and M. H. BOON, *Acta Metallurgica* **15** (1967) 958.
5. K. S. RAMAN, E. S. D. DAS, and K. I. VASU, *Current Sci.* **38** (1969) 130.
6. *Idem. J. Mater. Sci.* **5** (1970) 105.
7. W. DESORBO, H. N. TREAFTIS, and D. TURNBULL, *Acta Metallurgica* **6** (1958) 401.
8. E. S. D. DAS, K. S. RAMAN, and K. I. VASU, *Trans. Indian Inst. Metals* (In press).
9. A. J. PERRY and K. M. ENTWISTLE, *J. Inst. Metals* **96** (1968) 344.
10. M. OHTA, F. HASHIMOTO, and T. TANIMOTO, *Mem. of the School of Eng., Okayama Univ.* **3** (1968) 39.
11. M. OHTA and F. HASHIMOTO, *Trans. Japan. Inst. Met.* **6** (1965) 9.
12. A. FERARI, P. FIORINI, and F. GATTO, *Alumino* **36** (1967) 409.
13. J. TAKAMURA, in "Lattice Defects in Quenched Metals", edited by R. M. J. Cotterill, M. Doyama, J. J. Jackson, and M. Meshii (Academic Press, New York, 1965) 521.
14. F. CATTANEO and E. GERMAGNOLI, *Nouvo Cemento* **28** (1963) 923.
15. W. J. PLUMBRIDGE and K. M. ENTWISTLE, *J. Inst. Metals* **97** (1969) 232.
16. K. OKAZAKI and J. TAKAMURA, *Suiyokwai-Shi* **15** (1963) 89.
17. A. D. KING and J. BURKE, Conf. on "Point Defects in Metals" Reading Inst. Phys. (1967).
18. VAN DEN BEUKEL, *Phys. Stat. Solidi* **23** (1967) 165.
19. M. DOYAMA, *Phys. Rev.* **148** (1966) 681.
20. B. SPRUSIL and V. VALVODA, *Acta Metallurgica* **15** (1967) 1269.
21. D. R. BEAMAN, R. W. BALLUFFI, and R. O. SIMMONS, *Phys. Rev.* **134** (1964) A532.
22. *Idem, ibid* **137** (1965) A917.
23. E. S. D. DAS, K. S. RAMAN, and K. I. VASU, Paper to appear in *Trans. Japan Inst. Metal* (1971).
24. A. BLANDIN and J. L. DE'PLANTE, "Metallic Solid Solutions" (Benjamin, New York, 1963).
25. J. D. ESHELBY, *Acta Metallurgica* **3** (1955) 487.
26. L. PAULING, *J. Amer. Chem. Soc.* **69** (1947) 542.
27. K. S. RAMAN, E. S. D. DAS, and K. I. VASU, *Scripta Metallurgica* **4** (1970) 291.
28. M. OHTA and F. HASHIMOTO, *J. Phys. Soc. Japan* **19** (1964) 1987.
29. S. CERASARA, T. FEDERIGHI, and P. FIORINI, *Acta Metallurgica* **17** (1969) 225.
30. K. SHIMIZU and J. TAKAMURA, *Suiyokwai-Shi* **15** (1963) 95.
31. F. HASHIMOTO and M. OHTA, *J. Phys. Soc. Japan* **19** (1964) 1331.
32. T. FEDERIGHI, in "Lattice Defects in Quenched Metals" edited by R. M. J. Cotterill, M. Doyama, J. J. Jackson, and M. Meshii (Academic Press, New York, 1965) 217.
33. L. A. GIRIFALCO and H. HERMAN, *Acta Metallurgica* **13** (1965) 583.
34. D. TURNBULL, H. S. ROSENBAUM, and H. N. TREAFTIS, *ibid* **8** (1960) 277.
35. K. N. MURTY and K. I. VASU, *Mater. Sci. Eng.* **5** (1970) 235.
36. J. E. HILLIARD, B. L. AVERBACH, and M. COHEN, *Acta Metallurgica* **2** (1954) 621.
37. A. BEERWALD, *Z. Elektrochem.* **45** (1939) 789.

Received 13 April and accepted 19 July 1971.